Thermal radiation at high-temperature and high-pressure conditions: comparison of models for design and scale-up of entrained flow gasification processes

Maximilian Dammann*,,***, Marco Mancini***, Thomas Kolb*,** and Roman Weber*****

maximilian.dammann@kit.edu, maximilian.dammann@tu-clausthal.de

*Karlsruhe Institute of Technology (KIT), Engler-Bunte-Institute, Fuel Technology (EBI ceb), Engler-Bunte-Ring 1, 76131 Karlsruhe, Germany
**Karlsruhe Institute of Technology (KIT), Institute for Technical Chemistry, Gasification Technology (ITC vgt), Herrmann-von-Helmholtz-Platz 1, 76344 Eggenstein-Leopoldshafen, Germany
***Clausthal University of Technology, Institute for Energy Process Engineering and Fuel Technology (IEVB), Agricolastrasse 4, 38678 Clausthal-Zellerfeld, Germany

Abstract

Thermal radiation is an important sub-process in high-pressure entrained flow gasification. However, it was seldom investigated in previous CFD studies and was usually accounted for by common radiation and simplified gas radiation property models. Therefore, comparative radiation simulations were performed within this work and with respect to the bioliq Entrained Flow Gasifier (bioliq EFG) [1] of Karlsruhe Institute of Technology. The bioliq EFG operates at 40 bar and has got, contrary to other entrained flow gasifiers, a segmental cooling screen enabling local heat flux analysis [1]. This feature allows a unique comparison of experimental with numerical results; the latter were obtained by performing one-dimensional radiation and two-dimensional CFD simulations. The CFD simulations were carried out to investigate the performance of simplified gas radiation property models incorporated within the CFD model of the bioliq EFG [2], while the one-dimensional radiation simulations have enabled further comparison with the most recent developments for gas radiation property models. This paper reports on the simulation results and provides recommendations for the selection of gas radiation property models for CFD simulations with the discrete ordinates model and with emphasis on radiative heat transfer at high-pressure conditions. In case of largely isothermal and homogeneous conditions with exemption of the flame zone, weighted-sum-of-grey-gas models can be recommended to be used with the discrete ordinates model if user-defined weighted-sum-of-grey-gas models (i) are obtained from accurate line-by-line calculations, (ii) are based on conditions prevailing in the entrained flow gasifier and (iii) are applied using the non-grey or band approach. In absence of such weighted-sum-of-grey-gas models, spectral-line-weighted-sum-of-grey-gas models based on the latest tabulation [3] can be used instead. In addition to that, soot radiation becomes important at soot volume fractions above 10^{-6} and should be accounted for if such conditions are expected in entrained flow gasifiers.

Introduction

In entrained flow gasification processes, carbonaceous fuels are converted to synthesis gas at high-temperature and high-pressure conditions. Since the current fossil fuel-based technologies need to be replaced in the foreseeable future, new biomass-based technologies, as the bioliq® process [4], and new flowsheet and CFD models are under development [2, 5].

In the CFD models, thermal radiation is an important element since it is the dominant mode of heat transfer at high-temperature and high-pressure conditions due to large contents of water vapour, carbon dioxide and carbon monoxide. Appropriate mathematical description of thermal radiation is therefore required. However, previous CFD studies on entrained flow gasification relied on ready available absorption coefficient models. In addition to constant values [6] and polynomials [7], the weighted-sum-of-grey-gas (WSSG) model of Smith et al. [8], originally developed for atmospheric combustion conditions, was frequently used (e.g. [9, 10, 11, 12, 13, 14, 15, 16]) and combined with a mean beam length condition approach, as it is available by default in ANSYS Fluent [17]. More recent developments as spectral-line-weighted-sum-of-grey-gas (SLWSGG) models (e.g. [3]), full-spectrum *k* (FSK)

distributions (e.g. [18]) or improved WSGG models (e.g. [19]) were not applied since substantial efforts are required for their coupling with CFD.
Although WSGG models, SLWSGG models and FSK distributions differ, they rely on the absorption spectra of the gas molecules accounted for through appropriate line-by-line (LBL) calculations. The latter are performed using the available spectroscopic databases as HITEMP-2010 [20] and using the common line-shape functions, the Lorentz function or the Voigt function. Transmissivity spectra corresponding to such calculated absorption spectra are typically in very good agreement with the measured spectra at atmospheric pressure. However, at high-density conditions, the absorption coefficient in the line wings is overestimated due to imperfections of the line-shape functions. In order to minimise the discrepancies, Hartmann et al. [21, 22, 23], Pearson et al. [3] and Alberti et al. [24, 25, 26, 27] developed empirical correction methods. Hartmann et al. [21, 22, 23] tabulated χ-factors for specific temperature and wavenumber ranges. Pearson et al. [3] cut the H_2O lines after 2750 half-widths and the CO_2 and CO lines after 600 half-widths. Alberti et al. [24, 25, 26, 27] suggested cut-off criteria that take temperature and total pressure into account and are applicable for a wide range of temperatures and total pressures. The latter criteria were used to re-create emissivity charts and to develop customised weighted-sum-of-grey-gas models for atmospheric entrained flow gasification conditions [28] and high-pressure entrained flow gasification conditions [2]. The models were applied in RANS based CFD simulations, which demonstrated the dominant influence of thermal radiation on the heat removal. Possible simplifications were suggested for atmospheric conditions [28]. However, similar analysis has not yet been provided for high-pressure conditions. Therefore, this paper focuses on thermal gas radiation at high-temperature and high-pressure conditions and possible simplifications with respect to the bioliq Entrained Flow Gasifier (bioliq EFG) experiment V82.1 [2, 5]. To this end, comparative simulations were performed using a one-dimensional radiation model of a slab configuration and the two-dimensional CFD model of the bioliq EFG [2]. Gas radiation property models used have been based on LBL calculations, emissivity charts, WSGG models and SLWSGG models.

Experiments

The bioliq EFG experiment V82.1 focusses on the gasification of a model slurry consisting of 96 % ethylene glycol and 4 % A-Glass with oxygen and steam at a total pressure of 40 bar and a total thermal input of 5 MW [5]. Since the bioliq EFG is a membrane wall entrained flow gasifier that operates in slagging mode, the mineral compounds mainly deposit as slag on the refractory and flow down the cooling screen during operation. Mass or volume flow rates, temperatures and pressures of the inlet streams and the dry gas composition after the quench are recorded during operation and are the basis for process parameter calculations based on both elemental and energy balances and chemical equilibrium [5]. For the bioliq EFG experiment V82.1, Santo et al. [5] already provided the segmental heat removal, which is used as experimental basis for comparison within this paper.

LBL calculations

LBL calculations were performed using the HITEMP-2010 database [20] and the LBL software of Alberti et al. [24, 25, 26, 27] to obtain absorption spectra for specified gas pressures, gas temperatures and gas compositions with a spectral wavenumber range between $\eta_{min} = 0$ and $\eta_{max} = 30000$ cm^{-1}. In each LBL calculation, the spectral lines were determined using the Voigt function to a minimum absorption coefficient of 10^{-9} cm^{-1} and using a wavenumber discretisation of 0.01 cm^{-1}. Only contributions of H_2O, CO_2 and CO have been taken into account while contributions of CH_4 and OH have been neglected.

Emissivity charts

Emissivity charts for specified total gas pressures and gas compositions were created each using 46 absorption spectra obtained at 450 K, 500 K, …, 1950 K, 2000 K, 2100 K, …, 3000 K and using 30 pressure path lengths defined by logarithmic spacing between 0.001 bar cm and 6000 bar cm. The total emissivity ε_{tot} was calculated by

$$\varepsilon_{\mathrm{tot}} = \frac{\int_{\eta_{\mathrm{min}}}^{\eta_{\mathrm{max}}} \varepsilon_\eta \, \dot{e}_{\eta,\mathrm{b}}(\eta,T)\mathrm{d}\eta}{\int_{\eta_{\mathrm{min}}}^{\eta_{\mathrm{max}}} \dot{e}_{\eta,\mathrm{b}}(\eta,T)\,\mathrm{d}\eta}\,, \tag{1}$$

where ε_η is the spectral emissivity and $\dot{e}_{\eta,\mathrm{b}}$ is the Planck function. The spectral emissivity ε_η is defined by

$$\varepsilon_\eta = 1 - \exp\left(-K_\eta \, L\right)\,, \tag{2}$$

where K_η is the spectral absorption coefficient (as determined in the LBL calculations) and L is the path length.

Weighted-sum-of-grey-gas models

Two WSGG models were used in this work: (i) a user-defined model developed using a reference condition of the bioliq EFG experiment V82.1 and (ii) the model of Smith et al. [8].
The user-defined WSGG model was obtained by constrained non-linear multi-variable regression of the corresponding total emissivity chart using the expression

$$\varepsilon_{\mathrm{tot}} = \sum_{k=0}^{N_{\mathrm{gas}}} a_k\,(T)\left(1-\exp\left(-K_{p,k}\left(x_{\mathrm{H_2O}}+x_{\mathrm{CO_2}}\right)p_{\mathrm{tot}}\,L\right)\right), \tag{3}$$

where a_k and $K_{p,k}$ are the weight and the pressure-based absorption coefficient of pseudo-gas k, respectively. N_{gas} is the number of pseudo gases, x_{H2O} and x_{CO2} are the gas mole fractions of H_2O and CO_2, respectively, p_{tot} is the total pressure and L is the path length. The gas mole fraction of CO was not considered in this expression due to improved fitting results. The reason is that, although there is a relatively large amount of CO present in the gas phase, its contribution to the total emissivity $\varepsilon_{\mathrm{tot}}$ is relatively weak due to strong overlapping of the 4.7 µm band of CO with the 6.3 µm band of H_2O and the 4.3 µm band of CO_2.
In addition to the user-defined WSGG model, the WSGG model of Smith et al. [8] has been considered due to its popularity and its implementation in ANSYS Fluent [17]. This model had been generated from the exponential-wide-band model of Edwards and Modak [29, 30] for H_2O-CO_2-N_2 mixtures at a total gas pressure of 1 atm, at gas temperatures between 600 K and 2400 K and at typical gas combustion compositions. In ANSYS Fluent [17], it is combined with the scaling rules of Edwards and Matavosian [31] in order to estimate the total emissivity $\varepsilon_{\mathrm{tot}}$ at pressures up to 10 atm. The scaling rules were also used in this work.
WSGG models can be applied using different approaches. The most common are the reference condition (RC) approach and the mean beam length condition (MBC) approach. The RC approach is a band approach, i.e. pseudo-gases are assumed in the radiation simulations; furthermore, the WSGG model, obtained using a reference condition, is applied with the local gas condition. In contrast, the MBC approach is a grey approach. This means that the total emissivity $\varepsilon_{\mathrm{tot}}$ is firstly calculated using the local gas condition and Eq. (3); subsequently, a mean gas absorption coefficient $K_{\mathrm{gas,mean}}$ is estimated applying the relationship of Hottel and Sarofim [32]

$$K_{\mathrm{gas,mean}} = -\frac{\ln(1-\varepsilon_{\mathrm{tot}})}{L_{\mathrm{mean}}}, \tag{4}$$

where is L_{mean} is the mean path length. The mean path length L_{mean} is defined by 3.6 V / A_{s} for an arbitrary geometry with the volume V and the surface area A_{s} while it is given by 1.76 L for a slab configuration with the length L.

Spectral-line-weighted-sum-of-grey-gas models

SLWSGG models were applied in this work using the absorption line distribution function tabulation of Pearson et al. [3] and the multiplication method for mixtures.

Soot contributions

Soot contributions were approximated by the correlation proposed by Felske and Tien [33]. The average absorption coefficient of soot K_{soot} was accordingly described by

$$K_{\mathrm{soot}} = 3.72\, f_{\mathrm{v,soot}}\, k_{0,\mathrm{soot}}\, \frac{T}{C_2}, \tag{5}$$

where $f_{\mathrm{v,soot}}$ is the soot volume fraction, $k_{0,\mathrm{soot}}$ is the soot constant, T is the temperature and C_2 is 1.4387… · 10^{-2} m K.

CFD simulations

CFD simulations of the bioliq EFG experiment V82.1 were carried out using the mathematical model described by Dammann et al. [2], which is based on the RANS and the Euler-Lagrange approaches and a two-dimensional axis-symmetric geometry of the bioliq EFG. Turbulence and chemistry are taken into account by the standard k-ε model and the eddy-dissipation-concept model in combination with a global

reaction mechanism. Particles are injected consisting of liquid and solid fractions. While the liquid ethylene glycol fractions vaporise according to the classical convective vaporisation model, the solid A-Glass fractions are considered as inert. Slagging is implemented using a simplified slag flow model based on Seggiani [34]. Radiation is described using the discrete ordinates model with a solid angle discretisation of 4 x 8 x 8. The discrete ordinates model was used together with (i) the user-defined WSGG model and the RC approach or (ii) with the user-defined WSGG model and the MBC approach or (iii) with the scaled WSGG model of Smith et al. [8] and the MBC approach. Thus, three different models for the absorption coefficient were tested.

1D slab simulations

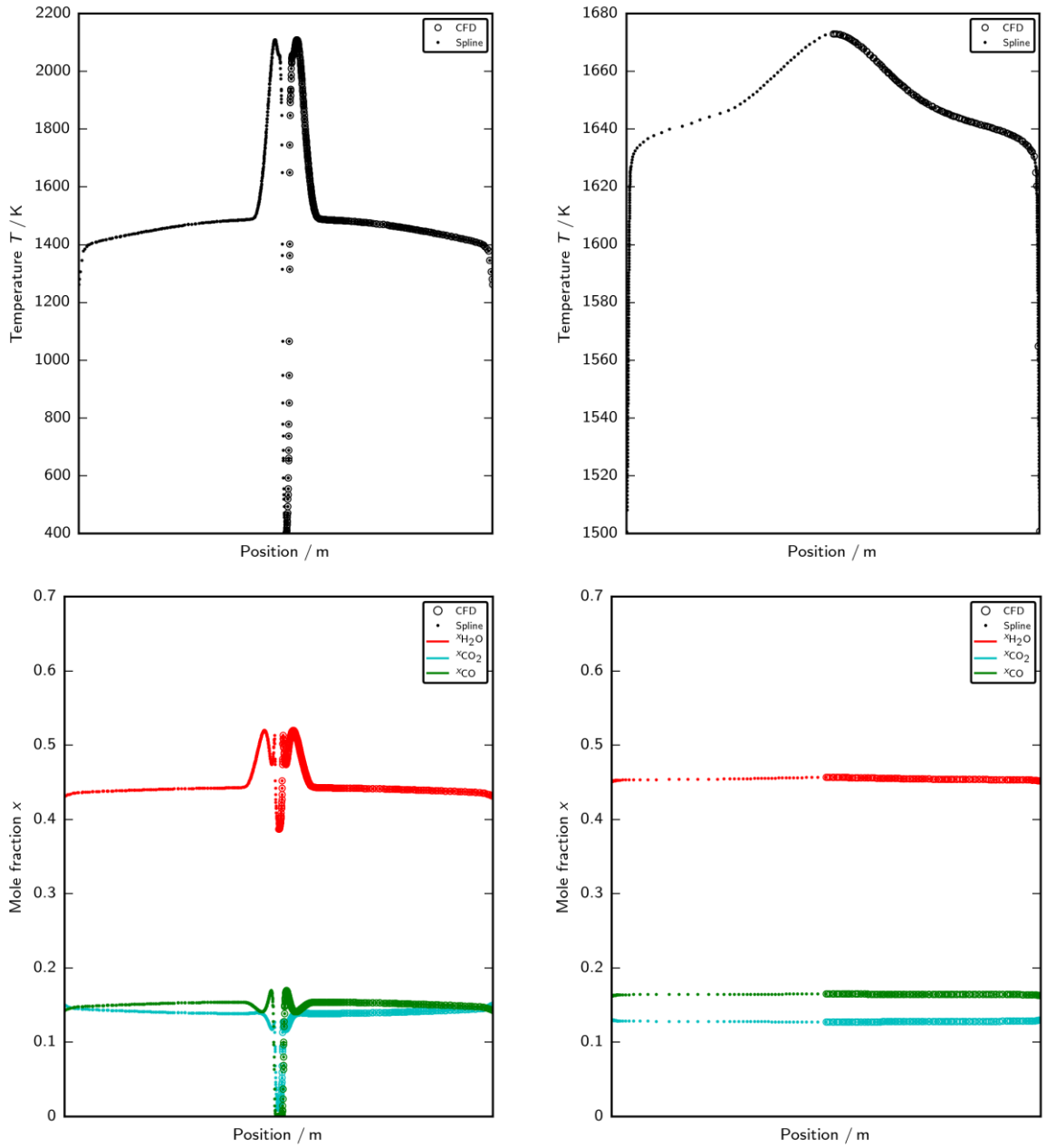

Figure 1. Gas temperature profiles (top) and gas mole fraction profiles (bottom) at burner distances of 260 mm (left) and 1524 mm (right).

1D slab simulations are concerned with the radiative heat transfer between two infinite parallel plates. In this work, such simulations were performed for two cases that are defined using gas temperature and gas concentration profiles extracted from the CFD simulation of the bioliq EFG experiment V82.1 (with

the user-defined WSGG model and the RC approach) at burner distances of 260 mm and 1524 mm. Extracted gas temperature and gas mole fraction profiles of H_2O, CO_2 and CO are shown as open circle markers in Fig. 1.
For the 1D slab simulations, the extracted profiles were mirrored and interpolated using splines. In case of the burner distance of 1524 mm, the splines were used to determine gas pressure, gas temperature and gas mole fraction profiles on a mesh with 319 nodes resolving the boundary layer. In case of the burner distance of 260 mm, the original mesh with 737 nodes was used.
For the gas condition at each node, absorption spectra were determined using LBL calculations. In this paper, these spectra represent the most accurate gas radiation property model, which has served as a reference model and is hereinafter referred as the LBL model. Additionally, the user-defined WSGG model combined with the RC or the MBC approach, the WSGG model of Smith et al. [8] combined with scaling rules of Edwards and Matavosian [31] and the MBC approach and SLWSGG models based on the tabulation of Pearson et al. [3] were used as basis for the 1D slab simulations. In these simulations, the radiative transfer equation

$$\frac{\mathrm{d}\, I_k}{\mathrm{d}\, s} + K_k\, I_k = K_k\, I_{\mathrm{b},k} \tag{6}$$

was solved for each band or gas k using the discrete ordinates model with 36 positive and 36 negative directions. Here, I_k is the intensity of band or gas k, K_k is the absorption coefficient of band or gas k, $I_{\mathrm{b},k}$ is the black-body intensity of band or gas k and s is the path length. Grey boundary conditions identical to those used in the CFD simulations were applied to solve the radiative transfer equations.

Results

Results from the 1D slab simulations are compared using the heat flux $\dot{q}$, which was obtained from the weighted summation over the net radiation intensities. In Fig. 2, the results from the 1D slab simulations at both burner distances are shown while the acronyms used in the legends are explained in Table 1.

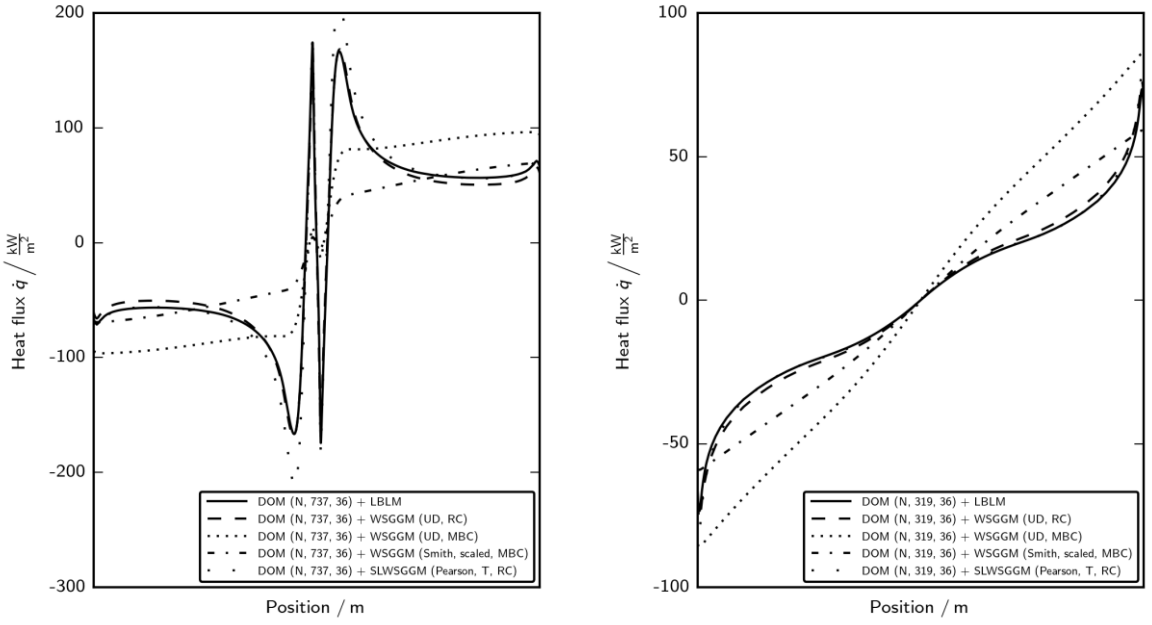

Figure 2. Comparison of heat flux profiles at burner distances of 260 mm (left) and 1524 mm (right) based on 1D slab simulations. Acronyms are explained in Table 1.

In comparison with the predictions based on the LBL model, both the user-defined WSGG model combined with the RC approach and the SLWSGG models perform very well. Thus, the heat source (not shown), which is the divergence of the heat flux, is accurately predicted. Large deviations are obvious for the predictions using those WSGG models that are combined with the MBC approach.
By comparison, the (radiation) boundary heat fluxes at 1524 mm are predicted quite well by all simplified models as shown in Table 2. Particularly, the scaled WSGG model of Smith et al. [8] is accurate realising that it was developed for atmospheric combustion conditions based on emissivity models that are

nowadays regarded as inaccurate. The good performance of the scaled WSGG model of Smith et al. [8] can be explained by the MBC approach. Even larger errors in the prediction of the total emissivity do not affect the mean absorption coefficient significantly. Therefore, the correct magnitude of the total emissivity is sufficient, which is granted by the scaled WSGG model of Smith et al. [8]. Recalling that the MBC approach was defined to provide good predictions of the wall heat fluxes only, this deficiency can clearly be seen in the predictions with the MBC approach in Fig. 2.

Table 1. Acronyms.

DOM	Discrete ordinates model
LBLM	Line-by-line model
WSGGM	Weighted-sum-of-grey-gas model
SLWSGGM	Spectral-line-weighted-sum-of-grey-gas model
RC	Reference condition approach
MBC	Mean beam length condition approach
N	Numerical solution approach
T	Tabulated approach
737 | 319	Number of nodes
36	Number of ordinates

Table 2. Radiation boundary heat fluxes at 1524 mm.

Simulation	Case	Heat flux $\|\dot{q}\|$ / kW/m²
1D slab	DOM + LBLM	66.3
1D slab	DOM + WSGGM (UD, RC)	69.7
1D slab	DOM + WSGGM (UD, MBC)	84.7
1D slab	DOM + WSGGM (Smith, scaled, MBC)	58.7
1D slab	DOM + SLWSGGM (Pearson, T, RC)	71.4
2D CFD	DOM + WSGGM (UD, RC)	75.7
2D CFD	DOM + WSGGM (Smith, scaled, MBC)	68.6

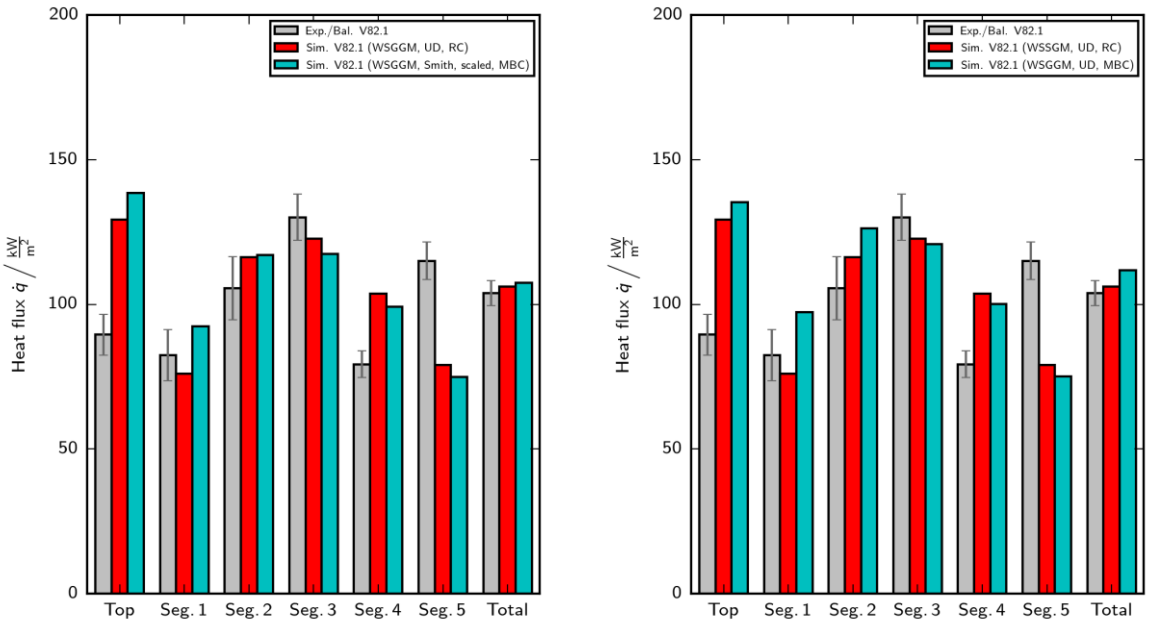

Figure 3. Comparison of the experimental and numerical results of the bioliq EFG experiment V82.1 concerning the segmental and total heat fluxes. Exp./Bal.: results based on measurements and balances [5]. Sim.: results based on CFD simulations. Further acronyms are explained in Table 1.

Results from the CFD simulations are compared using the segmental heat fluxes $\dot{q}$ in Fig. 3. CFD simulations were carried out (i) using the user-defined WSGG model and the band approach, (ii) using the user-defined WSGG model and the MBC approach and (iii) using the scaled WSSG model of Smith et al. [8] and the MBC approach, as it is implemented in ANSYS Fluent [17]. The results show only a

moderate impact of the gas radiation property model on the predictions of the boundary heat fluxes, which is in agreement with the results of the 1D slab simulations. However, the WSSG model combined with the band approach provides the best numerical results in comparison with the experimental results. Furthermore, the (radiation) boundary heat fluxes at the burner distance of 1524 mm were extracted from the CFD simulations and are presented in Table 2. In comparison with the heat fluxes predicted by the 1D slab simulations, similar predictions are made in values. This applies also for the burner distance of 260 mm (not shown). Thus, 1D slab simulations are a good alternative for radiation heat flux estimations if average gas conditions are known.

Discussion

bioliq EFG experiments with ethylene glycol at higher operating temperatures currently indicate low soot concentrations. Consequently, soot is neglected in the CFD model. However, soot measurements have not been carried out yet. It is thus informative to determine at what soot volume fraction the currently predicted heat fluxes would be substantially altered. To this end, the 1D slab model was used to examine the effect of both soot volume fraction and soot constant on the heat flux predictions. As shown in Fig. 4, while the soot constant does not impact the heat flux predictions, soot volume fractions above 10^{-6} significantly change the absorption and emission.

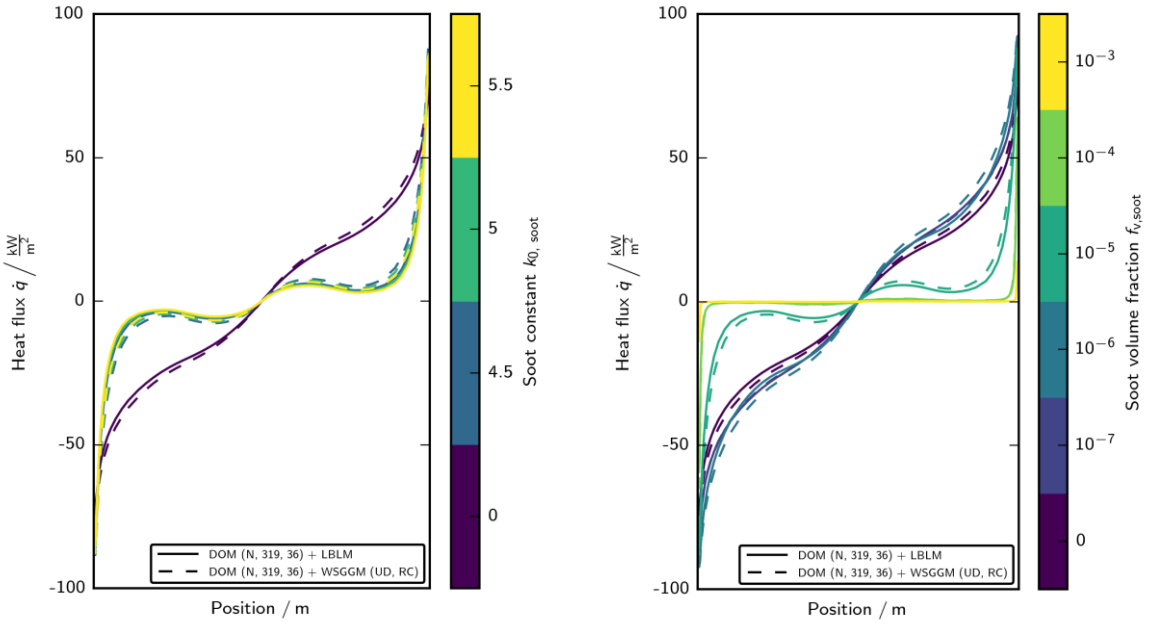

Figure 4. Comparison of heat flux profiles at the burner distance of 1524 mm based on 1D slab simulations for different soot constants at constant soot volume fraction (left) and for different soot volume fractions at constant soot constant (right). Acronyms are explained in Table 1.

Conclusions

Comparative one-dimensional slab and two-dimensional CFD simulations were performed in order to obtain an insight into thermal radiation at high-pressure entrained flow gasification conditions. Results show that simulations with a user-defined weighted-sum-of-grey-gas (WSGG) model and the band approach give accurate results if the WSGG model is generated using appropriate line-by-line calculations using HITEMP-2010 database [20]. Generation of such a WSGG model is an elaborative venture but it guarantees accurate predictions of the heat flux and the heat source. Spectral-line-weighted-sum-of-grey-gas models based on the latest tabulation of Pearson et al. [3] might be an alternative at the expense of increased number of pseudo gases. Reasonable predictions of the wall heat flux are also provided by the WSGG model of Smith et al. [8] combined with the mean beam length condition approach and the scaling rules of Edwards and Matavosian [31]. However, this model shows deficiencies in predicting the heat flux and the heat source distributions.

Since the bioliq EFG experiment with ethylene glycol at higher operating temperatures focussed in this paper demonstrated low soot concentrations, soot was neglected in the simulations. However, the influence of soot was investigated showing that its contribution has to be taken into account for soot volume fractions exceeding 10^{-6}.

Acknowledgements

The authors thank (i) Michael Alberti (formerly Clausthal University of Technology, Institute for Energy Process Engineering and Fuel Technology) and John T. Pearson (formerly Brigham Young University, Department of Mechanical Engineering) for their preceding works and (ii) David Böning, Mark Eberhard, Ulrike Santo and Hannah Schmid (Karlsruhe Institute of Technology, Institute for Technical Chemistry, Gasification Technology) for the constant collaboration.

References

[1] Eberhard, M., Santo, U., Michelfelder, B., Günther, A., Weigand, P., Matthes, J., Waibel, P., Hagenmeyer, V., Kolb, T., "The bioliq® Entrained Flow Gasifier: a model for the German Energiewende", *ChemBioEng Reviews*, 7, 2020, 106-118.

[2] Dammann, M., Mancini, M., Weber, R., Kolb, T., "Entrained flow gasification: mathematical modelling based on RANS for design and scale-up", *30. Deutscher Flammentag: Verbrennung und Feuerung*, Hannover-Garbsen, Germany, 2021.

[3] Pearson, J. T., Webb, B. W., Solovjov, V. P., Ma, J., "Efficient representation of the absorption line blackbody distribution function for H_2O, CO_2, and CO at variable temperature, mole fraction, and total pressure", *Journal of Quantitative Spectroscopy and Radiative Transfer*, 138, 2014, 82-96.

[4] Dahmen, N., Abeln, J., Eberhard, M., Kolb, T., Leibold, H., Sauer, J., Stapf, D., Zimmerlin, B., "The bioliq process for producing synthetic transportation fuels", *WIREs Energy Environment*, 6, 2016.

[5] Santo, U., Böning, D., Eberhard, M., Schmid, H., Kolb, T., "Entrained flow gasification: experiments and balancing for design and scale-up", *30. Deutscher Flammentag: Verbrennung und Feuerung*, Hannover-Garbsen, Germany, 2021.

[6] Marklund, M., "Pressurized entrained-flow high temperature black liquor gasification: CFD based reactor scale-up method and spray burner characterization", *Ph.D. thesis*, Department of Engineering Sciences and Mathematics, Luleå University of Technology, Luleå, Sweden, 2006.

[7] Lu, X., Wang, T., "Investigation of radiation models in entrained-flow coal gasification simulation", *International Journal of Heat and Mass Transfer*, 67, 2013, 377-392.

[8] Smith, T. F., Shen, Z. F., Friedman, J. N., "Evaluation of coefficients for the weighted sum of gray gases model", *Journal of Heat Transfer*, 104, 1982, 602-608.

[9] Jeong, H. J., Hwang, I. S., Park, S. S., Hwang, J., "Investigation on co-gasification of coal and biomass in Shell gasifier by using a validated gasification model", *Fuel*, 196, 2017, 371-377.

[10] Ma, J., Zitney, S. E., "Computational fluid dynamic modeling of entrained-flow gasifiers with improved physical and chemical submodels", *Energy & Fuels*, 26, 12, 2012, 7195-7219.

[11] Park, S., Jeong, H., Hwang, J., "3-D CFD modeling for parametric study in a 300-MW one-stage oxygen-blown entrained-bed coal gasifier", *Energies*, 8, 2015, 4216-4236.

[12] Rashidi, A., "CFD simulation of biomass gasification using detailed chemistry", *Ph.D. thesis*, Naturwissenschaftlich-Mathematische Gesamtfakultät der Ruprecht-Karls-Universität Heidelberg, Heidelberg, Germany, 2011.

[13] Sun, Z., Dai, Z., Zhou, Z., Guo, Q., Yu, G., "Numerical simulation of industrial opposed multiburner coal-water slurry entrained flow gasifier", *Industrial & Engineering Chemistry Research*, 51, 2012, 2560-2569.

[14] Tominaga, H., Yamashita, T., Ando, T., Asahiro, N., "Simulator development of entrained flow coal gasifiers at high temperature and high pressure atmosphere", *IFRF Combustion Journal*, 2000, 1-22.

[15] Vascellari, M., Roberts, D. G., Hla, S. S., Harris, D. J., Hasse, C., From laboratory-scale experiments to industrial-scale CFD simulations of entrained flow coal gasification, *Fuel*, 152 2015, 58-73.

[16] Wang, L., Jia, Y., Kumar, S., Li, R., Mahar, R. B., Ali, M., Unar, I. N., Sultan, U., Memon, K., "Numerical analysis on the influential factors of coal gasification performance in two-stage entrained flow gasifier", *Applied Thermal Engineering*,112, 2017, 1601-1611.

[17] ANSYS, "ANSYS Fluent theory guide. Release 2020 R2", *SAS*, 2020.

[18] Wang, C., Modest, M. F., He, B., "Full-spectrum correlated-*k*-distribution look-up table for radiative transfer in nonhomogeneous participating media with gas-particle mixtures", *International Journal of Heat and Mass Transfer*, 2019, 137, 1053-1063.

[19] Coelho, F. R., Franca, F. H. R., "WSGG correlations based on HITEMP 2010 for gas mixtures of H_2O and CO_2 in high total pressure conditions", *International Journal of Heat and Mass Transfer*, 2018, 127, 105-114.

[20] Rothman, L. S. et al.: “The HITRAN 2008 molecular spectroscopic database”, *Journal of Quantitative Spectroscopy and Radiative Transfer*, 2009, 110, 533-572.
[21] Perrin, M. Y., Hartmann, J. M., “Temperature-dependent measurements and modeling of absorption by CO_2-N_2 mixtures in the far line-wings of the 4.3 µm CO_2 band”, *Journal of Quantitative Spectroscopy and Radiative Transfer*, 1989, 42, 311-317.
[22] Hartmann, J. M., Perrin, M. Y., Ma, Q., Tippings, R. H., “The infrared continuum of pure water vapor: Calculations and high-temperature measurements”, *Journal of Quantitative Spectroscopy and Radiative Transfer*, 1993, 49, 675-691.
[23] Brodbeck, C., Bouanich, J. P., Van-Thanh, N., Hartmann, J. M., Khalil, B., Le Doucen, R., “Absorption of radiation by gases from low to high pressures. II. Measurements and calculations of CO infrared spectra”, *Journal de Physique II, EDP Sciences*, 1993, 4, 2101-2118.
[24] Alberti, M., Weber, R., Mancini, M., “Re-creating Hottel's emissivity charts for carbon dioxide and extending them to 40 bar pressure using HITEMP-2010 data base”, *Combustion and Flame*, 162, 2015, 597-612.
[25] Alberti, M., Weber, R., Mancini, M., “Re-creating Hottel's emissivity charts for water vapor and extending them to 40 bar pressure using HITEMP-2010 data base”, *Combustion and Flame*, 169, 2016, 141-153.
[26] Alberti, M., Weber, R., Mancini, M., “Absorption of infrared radiation by carbon monoxide at elevated temperatures and pressures: Part A. Advancing the line-by-line procedure based on HITEMP-2010”, *Journal of Quantitative Spectroscopy and Radiative Transfer*, 200, 2017, 258-271.
[27] Alberti, M., Weber, R., Mancini, M., “Gray gas emissivities for H_2O-CO_2-CO-N_2 mixtures”, *Journal of Quantitative Spectroscopy and Radiative Transfer*, 219, 2018, 274-291.
[28] Mancini, M., Alberti, M., Dammann, M., Santo, U., Eckel, G., Kolb, T., Weber, R., “Entrained flow gasification. Part 2: mathematical modeling of the gasifier using RANS method”, *Fuel*, 225, 2018, 596-611.
[29] Edwards, D. K., “Molecular gas band radiation”, *Advances in Heat Transfer*, 1976, 115-193.
[30] Modak, Ashok T., “Exponential wide band parameters for the pure rotational band of water vapor”, *Journal of Quantitative Spectroscopy and Radiative Transfer*, 21, 1979, 131-142.
[31] Edwards, D. K., Matavosian, R., “Scaling rules for total absorptivity and emissivity of gases”, *Journal of Heat Transfer*, 106, 1984, 684-689.
[32] Hottel, H. C., Sarofim, A. F., Radiative Transfer”, *McGraw Hill*, New York, NY, USA, 1967.
[33] Felske, J. D., Tien, C. L, “The use of the Milne–Eddington absorption coefficient for radiative heat transfer in combustion systems”, *ASME Journal of Heat Transfer*, 9, 1977, 458-465.
[34] Seggiani, M., “Modelling and simulation of time varying slag flow in a Prenflo entrained-flow gasifier”, *Fuel*, 77, 1998, 1611-1621.